Functional Materials 11, No.1 (2004)

On contamination of lithium tetraborate single crystals with platinum (container material)

V.M.Holovey, O.O.Parlag, V.T.Maslyuk, P.P.Puga, M.M.Birov, D.O.Santoniy

Institute of Electron Physics, National Academy of Sciences of Ukraine,
21 Universitetska St., 88000 Uzhgorod, Ukraine

Received May 15, 2003

To determine trace quantities of platinum (i.e. containing material) in lithium tetraborate $Li_2B_4O_7$ single crystals, the photo-nuclear analysis method has been used by means of an M-30 electron accelerator. No platinum was found in the upper part of single crystals. i.e. its content is below the method sensitivity threshold (10^{-4} mass. %), whereas in the defect parts, it is $(1.86–8.20)\cdot10^{-4}$ mass. %. At low platinum levels in the melt, as well as low growth rates, almost no platinum was found in the upper crystals parts, while it is concentrated mainly in the bottom parts that contains gas and solid phase inclusions and blocks, i.e. during growth an effective Pt concentrating occurs.

Для определения следовых количеств платины (материала контейнера) в монокристаллах тетрабората лития $Li_2B_4O_7$ использован метод фотоядерного анализа с применением электронного ускорителя микротрона М-30. В верхней части монокристаллов платина не обнаружена, т.е. ее содержание находится ниже предела чувствительности метода (10^{-4} масс %), а в нижней дефектной части оно составляет $(1.86–8.20)\cdot10^{-4}$ масс.%. При низком содержании платины в расплаве, а также малых скоростях роста она практически отсутствует в верхних частях кристаллов и сосредоточивается преимущественно в их нижних частях, которые содержат газовые и твердофазные включения и блоки, т.е. в процессе роста происходит ее эффективное концентрирование.

Lithium tetraborate $Li_2B_4O_7$ (LTB) single crystals are the promising material for different opto- and acousto-electronics applications. This is due to such LTB properties as high transparency in visible and UV spectral regions [1], generation possibility of fourth and fifth harmonics [2, 3], high mechanical and radiation stability [4–6], low propagation rate of surface acoustic wave [7, 8], large electromechanical coupling ratio and presence of a direction with zero temperature expansion coefficient [9]. LTB doped with different impurities (in particular, copper or manganese) is also used in thermoluminescent dosimetry of X-ray, γ-, neutron (n), and mixed γ–n radiation [10].

Doping makes it possible to enlarge the material application range, while the presence of excess number of uncontrolled impurities could substantially worsen its operation characteristics, first of all, in fields related to the use of luminescent properties, in particular, in dosimetry. Since for LTB synthesis and single crystal growth platinum crucibles are usually used, the partial corrosion products of container material could be one of the possible sources of the above impurities. According to [11] where the single crystals were produced by Czochralski technique, at pulling rates above 1 mm/h the cellular growth was noticed resulting from impurity accumulation at the crystal-melt interface. In addition, platinum

dendrites oriented along the pulling direction were formed at some cell boundaries.

Such metallic platinum inclusions of 0.2 μm or smaller size were also observed in the defect parts of single crystals of lithium triborate LiB_3O_5 (LBO) [12], which is formed, like LTB, at the quasi-binary Li_2O–B_2O_3 section. The authors believe that the source of platinum is partial corrosion of the crucible due to the interaction of lithium carbonate Li_2CO_3 and lithium oxide Li_2O formed during LBO synthesis (at Li_2CO_3 thermal decomposition) with crucible walls. It should be noted that in both cases, platinum in the borate single crystals was formed a second phase (metal) and could be detected by optical methods. In this connection, the development of high-sensitivity methods for platinum impurity determination at different stages of LTB single crystal production, including the crystal parts which do not contain solid-phase inclusions, remains still an actual problem.

LTB was synthesized from the high-purity (12-3 grade) boron oxide B_2O_3 and high-purity (20-2 grade) lithium carbonate Li_2CO_3 in platinum crucibles (60 mm diameter and 50 mm high) in air according to the procedure described in [13]. The synthesis product was used as the initial raw material to grow single crystals without the crucible refilling. To compensate boron oxide losses due to incongruent LTB evaporation [14, 15] the oxide excess (up to 0.5 mol.%) was added to the initial mixture. LTB single crystals were grown by Czochralski method at the HX-620 apparatus along the [100] and [001] directions. The pulling rate was 3 to 6 mm/day and rotation speed, 4 to 10 rpm. During growth process, (melt contact with crucible lasted for about 150 hours) the melt temperature was 915 to 850°C, and the melt/crucible wall contact area was varied from 100 to 75 cm^2. The diameter 35 mm crystals produced had the fully transparent upper part with no second phase inclusions; no cellular growth areas with metal platinum inclusions at the dendrite boundary (similar to those in [11]) were noticed. Platinum content was determined separately in the upper transparent part, bottom defect part and also in the residual unused raw material in the crucible.

To determine the trace platinum amounts in LTB, the radioactivation analysis method was used. One of its principal advantages is the possibility to use the samples of relatively large (dozens of grams) mass, that allows the impurity determination threshold to be lowered considerably. The analysis

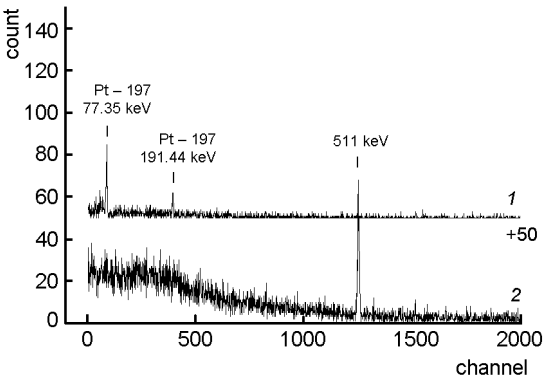

Fig. 1. Typical γ-spectrum of irradiated LTB samples and Pt-monitor, *1* – Pt-monitor, *2* – LTB.

was performed by a relative method, i.e. a reference sample was irradiated together with that under study. Both references and analyzed samples were activated and the induced activity was measured in the same geometric conditions and time intervals.

The activated samples were analyzed taking into account the nuclear physical properties of the LTB matrix elements (Li, B, O). As to the matrix elements, no γ-emission was found at the onset of measurements [16–18]. The reference samples were produced so as to minimize the systematic error due to their distinctions from the samples under study. The activation conditions excluded the error resulting from the influence of side nuclear reactions of the isotope under identification. Container material for both samples and references did not affect the determination error, while the relative error due to the thermal neutron flow density caused by distortions introduced by the samples under study, deceleration and construction materials as well as by their self-screening in the samples did not exceed 5 %. Irradiation was carried out using the electron accelerator at the Institute of Electron Physics, National Academy of Sciences of Ukraine (an M-30 microtron) in the standard geometric conditions at average current of about 5 to 10 μA and maximum electron energy of 12 MeV. During activation, the samples were placed in the irradiation unit that contained a 4 mm thick bremsstrahlung target mounted on the accelerated electron beam axis inside the PE moderator of 4π-configuration.

The measurements were carried out using the SBS-40 gamma-spectrometric complex comprising a semiconductor Ge(Li) detector of 100 cm^3 effective volume. The spectrometer resolution was about 3 keV

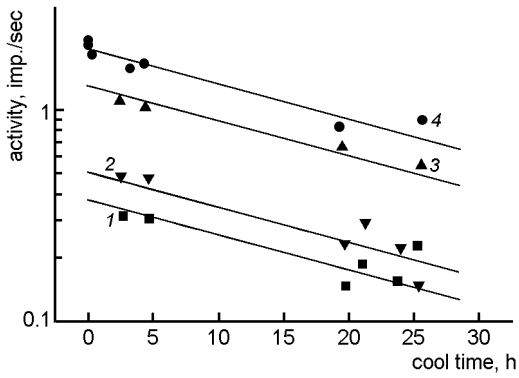

Fig. 2. Dependence of emission intensity for different mass Pt-containing monitors as a function of cooling time. Pt-etalons: experiment: *1* – M=0.0065 g, *2* – M=0.0091 g, *3* – M=0.0220 g, *4* – M=0.0376 g. Theory: lines.

for the 1333 keV Co–60 line, parameter drift of main characteristics (efficiency, peak-to-compton ratio, and resolution) did not exceed 1 %. The nuclear physical characteristics of the reactions of Pt–197 formation are presented in Table 1, while the principal experimental results, in Table 2. Fig. 1 shows typical gamma-spectra of irradiated LTB samples and Pt reference, the Pt-monitor sample activity as the function of cooling time is illustrated in Fig. 2.

The total statistical error of measurements was not higher than 10 %. A valid determination limit of Pt impurity in the above conditions was $(4–10)\cdot10^{-5}$ g [19]. This limit can be reduced by several times by increasing the sample mass. However, an excessive increase of mass is not expedient due to the increase of errors resulting from the flow density inhomogeneity of thermal neutrons, their self-screening in the samples under activation and γ-quanta self-absorption in analytical lines.

No platinum was detected in the upper high-quality part of LTB single crystals, because its content is below the sensitivity threshold of the method (10^{-4} mass. %). Platinum content in the bottom crystal part is $(1.86–8.20)\cdot10^{-4}$ mass. % and that in the residual raw material after growth process termination is $(5.38–35.40)\cdot10^{-4}$ mass. %. The interval of the limiting Pt content values for the bottom part of single crystal and raw material residuals is presented in Table 2. It characterizes the scatter of average content values obtained in a series of measurements carried out for five growth runs. As follows from the experimental data, the effective Pt distribution ratio is substantially less than unit (~0.1).

According to [20], the LTB crystal structure is based on the anion sublattice produced by 3D grid of boron-oxygen triangles and tetrahedrons. The grid includes channels oriented along the [001] crystallographic direction and containing tetrahedrally coordinated lithium ions. Electron density peaks in the B–O and Li–O bonds are shifted towards oxygen, i.e. the chemical bonding is of ion-covalent type. The impurities substituting lithium ions as well as

Table 1. Characteristics of Pt in nuclear reactions

Isotope	Abundance, mass %	Nuclear reaction	Cross section, B	Half-life, h
Pt–198	7.90	Pt–198(γ,*n*)Pt–197	$5.04\cdot10^{-1}$	18.0
Pt–198	7.90	Pt–198(*n*,2*n*)Pt–197	$2.3\cdot10^{3}$	18.0
Pt–196	25.30	Pt–196(n_{th},γ)Pt–197	$8.7\cdot10^{2}$	18.0

Table 2. Characteristics of measurement series

Sample	Residuals in a crucible after single crystal growth run	Lower part of single crystal
Weight, g	4.4065	6.5773
Beam parameters	E = 12 MeV i = 5–10 μA	E = 12 MeV i= 5–10 μA
Activation time, h	3.0	3.0
Cooling time, h	2.43–23.00	0.40–23.75
Measuring time, h	1–3	1–2
Number of measuring series, h	2	2

those located in the interstitials can be assumed to enter the LTB crystal structure most easily. Therefore, the main role in this case is played by the substituting ion dimensional factor and charge. According to the crystal-chemical ion radii table [21], constructed with under taking into account electron density of chemical bonding in the compounds with ion-covalent bond, this factor for tetrahedrally coordinated Li^+ is 0.73 Å. It should be noted that the substitution solid solution formation is the more probable, the closer are the dimensions of the ion under substitution and of the impurity ion [21]. Another essential factor affecting the impurity introduction is the charge of substituting ion and that of substituted one. Although the Pt ion radius is, according to [21], 0.74 Å and differs slightly from Li one, the Pt ion is multicharged. This circumstance hampers its introduction to the LTB crystalline lattice and results in a considerable Pt segregation during the growth process. At low platinum content in the melt, as well as at low growth rates, almost no platinum is found in the upper crystal part while it is concentrated mainly in the bottom part of the crystal that contains gas and solid inclusions and blocks, i.e. effective Pt concentrating occurs during growth. In the high-quality part containing no second phase inclusions, platinum content is at the level not exceeding the method sensitivity threshold. According to the results obtained, when studying thermostimulated luminescence in the high-quality part of undoped LTB single crystal, its intensity exceeds only slightly the background values [22] that also could testify a very low content of uncontrolled impurities.

Since chemical destruction of the crucible could occur due to the interaction of the lithium carbonate and oxide (resulting from the carbonate thermal decomposition) with the crucible walls during LTB synthesis, we have suggested, in order to reduce corrosion, the inner wall protection method based on formation of a coating from the presynthesized LTB [23]. At the repeated use of platinum crucibles, their partial mechanical destruction takes place accompanied by formation of a layer of fine-dispersed metallic platinum particles on the inner surface. These particles are aggregated mainly in the raw material residuals, since their transfer to the crystal-melt interface is hindered due to the high melt viscosity [24].

This work has been carried out under the support of the STCU Project # 2172.

References

1. T.Sugawara, R.Komatsu, S.Uda, *Solid State Communs.*, **107**, 233 (1998).
2. R.Komatsu, T.Sugawara, K.Sassa et al., *Appl. Phys. Lett.*, **70**, 3492 (1997).
3. R.Komatsu, T.Sugawara, N.Watanabe et al., *Rev. Laser Enging.*, **27**, 541 (1999).
4. A.O.Matkovskii, D.Yu.Sugak, Ya.V.Burak et al., *Rad. Effects and Defects in Solids*, **132**, 371 (1994).
5. G.I.Malovichko, L.E.Vitruk, N.Yu.Yurchenko et al., *Fiz. Tverd. Tela*, **34**, 509 (1992).
6. Ya.V.Burak, B.N.Kopko, I.T.Lyseiko et al., *Izv. AN SSSR. Neorg. Mater.*, **25**, 1226 (1989).
7. M.Adachi, K.Nakazawa, A.Kawabata, *Ferroelectrics*, **195**, 123 (1997).
8. A.E.Aliev, Ya.V.Burak, V.V.Vorob'ev et al., *Fiz. Tverd. Tela*, **32**, 2826 (1990).
9. K.Fukuta, J.Ushizawa, H.Suzuki et al., *Jap. J. Appl. Phys.*, **22–2**, 140 (1983).
10. S.W.S.McKeever, M.Moscovitch, P.D.Townsend, Thermoluminescence Dosimetry Materials: Propertries and Uses, Nuclear Technology Publ., Ashford (1995).
11. R.Komatsu, S.Uda, *Materials Research Bull.*, **33**, 433 (1998).
12. D.P.Shumov, A.T.Nenov, D.D.Nihtianova, *J. Cryst. Growth*, **169**, 519 (1996).
13. I.I.Turok, V.M.Holovey, P.P.Puga, Ukr. Pat. Appl. No.32242.
14. K.Tada, M.Tatsumi, Ya.Namikawa, Japan Pat. Appl. No.62-108800.
15. D.S.Robertson, Y.M.Young, *J. Mater. Sci.*, **17**, 1729 (1982).
16. Gamma-Ray Data For Neutron Activation Analysis (1999). http://www.nuc.bercley.edu/dept/courses/Ne104A/Gamma-search.html
17. Tables of Nuclear Data, Nuclear Data Center, Japan Atomic Energy Research Institute (1999). http://www.ndc.tocaj.jaeri.go.jp./NuC/
18. G.L.Molnar, Nuclear Data For Activation Analysis (1999). http://www/iki/kfki/hu/nuclear
19. V.T.Tustanovsky, Estimation of Activation Analysis Accuracy and Sensitivity, Atomizdat, Moscow (1976) [in Russian].
20. E.S.Radaev, L.A.Muradian, L.F.Malakhova et al., *Kristallografia*, **34**, 1400 (1989).
21. B.K.Vainstein, V.M.Fridkin, V.L.Indenbom, Modern Crystallography, Nauka, Moscow, **4**, (1979), p.75–81 [in Russian].
22. P.P.Puga, B.M.Hunda, *Uzhhorod Univ. Sci. Herald*, **8**, 115 (2000).
23. V.M.Holovey, I.I.Turok, P.P.Puga, Ukr. Pat. Appl. No.42149.
24. J.Liebertz, *Progr. Crystal Growth and Charact.*, **6**, 361 (1983).

Про входження платини (матеріалу контейнера) у монокристали тетраборату літію

В.М.Головей, О.О.Парлаг, В.Т.Маслюк, П.П.Пуга, М.М.Биров, Д.О.Сантоний

Для визначення слідових кількостей платини (матеріалу контейнера) у монокристалах тетраборату літію $Li_2B_4O_7$ використано метод фотоядерного аналіза з застосуванням електронного прискорювача мікротрона М-30. У верхній частині монокристалів платину не виявлено, тобто її вміст знаходиться нижче межі чутливості метода (10^{-4} мас %), а у нижній дефектній частині він складає $(1.86–8.20)\cdot10^{-4}$ ваг %. При низькому вмісті платини у розплаві, а також малих швидкостях росту вона практично відсутня у верхніх частинах кристалів і концентрується переважно в їхніх нижніх частинах, що містять газові і твердофазні включення та блоки, тобто в процесі росту відбувається її ефективне концентрування.